

Article

Study on the Tribological Characteristics of Australian Native First Generation and Second Generation Biodiesel Fuel

Md Mofijur Rahman *, Mohammad Rasul and Nur Md Sayeed Hassan

School of Engineering and Technology, Central Queensland University, Rockhampton, Queensland 4702, Australia; m.rasul@cqu.edu.au (M.R.); n.hassan@cqu.edu.au (N.M.S.H.)

* Correspondence: m.rahman@cqu.edu.au; Tel: +61-469851901

Academic Editor: Thomas E. Amidon

Received: 11 October 2016; Accepted: 22 December 2016; Published: 5 January 2017

Abstract: Biodiesels are a renewable energy source, and they have the potential to be used as alternatives to diesel fuel. The aim of this study is to investigate the wear and friction characteristics of Australian native first generation and second generation biodiesels using a four-ball tribo tester. The biodiesel was produced through a two-step transesterification process and characterized according to the American Society for Testing and Materials (ASTM) standards. The tribological experiment was carried out at a constant 1800 rpm and different loads and temperatures. In addition, the surface morphology of the ball was tested by scanning electron microscope (SEM)/energy dispersive X-ray spectroscopy (EDX) analysis. The test results indicated that biodiesel fuels have a lower coefficient of frictions (COF) and lower wear scar diameter (WSD) up to 83.50% and 41.28%, respectively, compared to conventional diesel fuel. The worn surface area results showed that biodiesel fuel has a minimum percentage of C and O, except Fe, compared to diesel. In addition, the worn surface area for diesel was found (2.20%–27.92%) to be higher than biodiesel. The findings of this study indicated that both first and second generation biodiesel fuels have better tribological performance than diesel fuel, and between the biodiesel fuels, macadamia biodiesel showed better lubrication performance.

Keywords: renewable energy; wear and friction; beauty leaf biodiesel; macadamia biodiesel

1. Introduction

Biodiesel is a most promising alternatives to fossil fuel as it can play a significant role in fulfilling the energy demand and lowering the greenhouse gas emissions into the environment [1,2]. Biodiesel is produced from plant oils [3] and animal fats through transesterification reactions [4–6]. Biodiesel is gaining popularity these days due to having some superior qualities to fossil diesel fuels such as renewability [7], biodegradability [8], higher flash point [9], cetane number [10], lubricity and less greenhouse gas emissions like CO, HC, PM, etc. [11]. In spite of having these positive aspects, biodiesel also has some shortcomings that restrain its commercialization [12,13]. The major drawbacks of biodiesel are that it causes injector coking, carbon deposition, oxidation and corrosion due to the presence of higher unsaturated fatty acids in its structure [14,15]. Subsequently, these problems may lead to the friction and wear in different moving components such as cylinder liners, bearings, cams, tappets, crankshaft journals, pistons and piston pins, valve guides, valve systems, etc. [16]. As mentioned earlier, biodiesel has higher lubricity than diesel fuel [17] and lubricity on the sliding components is delivered from the fuel itself. Biodiesel has better lubricity, which is affected by the oxidation formation, sulfur content, temperature, load, moisture absorption, and so on. Therefore, it is imperative to understand the wear and friction characteristics of each biodiesel in detail before

using it as an alternative to diesel fuel in the engines. For this reason, several laboratory tests have been performed by some researchers [18–21] with a four-ball wear machine, pin-on-disk wear testing machine and reciprocating wear tester to get an idea about the tribological behavior of biodiesel fuel.

For example, Ozioko [18] investigated the wear rate of carbon steel and aluminum alloy using *Moringa oleifera* oil with commercial lube oil by the pin-on-disc method at different load conditions. Their findings indicated that the wear rate increases with the load and 10% moringa oil with 90% lube oil showed a better lubrication performance that protects the metal-to-metal contact surfaces. Sharma et al. [19] studied the lubrication performance of *Moringa Oleifera* oil using the high-frequency reciprocating rig (HFRR) method and compared it with *Jatropha* oil, cottonseed oil, canola oil and sunflower oil. They found that *M. oleifera* oil is more suitable to use as a multi-grade lubricant compared to other oils. Fazal et al. [20] found that palm biodiesel has better lubricant properties than diesel fuel. In addition, the friction and wear decrease with increasing the percentages of palm biodiesel in the blend at different speeds and constant load (40 kg) and temperature (75 °C). Temperature is another crucial factor for the lubrication, which increases the friction and wears in the sliding components [16]. Habibullah et al. [21] found that 20% *Calophyllum* biodiesel blends have a better lubrication performance than diesel and other blends at different loads (40 kg, 50 kg, 63 kg and 80 kg) at a constant speed (1800 rpm) and room temperature using a four-ball tribotester. Each biodiesel fuel showed lower friction and wear characteristics than low sulfur fuels [22]. The lubrication performance of *Jatropha* biodiesel blends increases with increasing the percentages of biodiesel in the blend, and the *Jatropha* biodiesel showed better lubricity at lower load and temperature conditions [23]. Maru et al. [24] found lower frictional coefficients than diesel fuel when they investigated the lubrication properties of soybean and animal fats biodiesel by the HFRR method. Sulek et al. [25] reported that 5% and 100% rapeseed biodiesel lowers the frictional coefficient by 20% and 30% more, respectively, than diesel fuel. All of their observations indicated that the tribological properties of biodiesel fuels are influenced by different factors such as temperature, oxidation and moisture absorption.

Though some studies are available in this field, no report has been found in the literature on the tribological behavior of Australian native first generation macadamia oil biodiesel. Thus, there is a need to conduct further systematic research confirming the tribological behavior of different biodiesel fuels. Therefore, the aims of the present study are to characterize the lubricity regarding friction and wear for Australian native first generation macadamia biodiesel compared to that of second generation beauty leaf biodiesel as well as the conventional diesel fuel.

2. Description of Beauty Leaf and Macadamia Biodiesel Feedstocks

Beauty leaf is a versatile tree, and it is a member of the mangosteen family. It is non-invasive, tolerates harsh environmental conditions (acidity, salinity, and drought), and requires little maintenance [26]. Beauty leaf is a native Australian tree and has many attributes to be used as a biodiesel feedstock. It is mainly found in the regional areas of the Queensland and Northern territory states. It is also found in Indonesia, India, and Sri Lanka [27]. However, the plantlets of Australian origin seem to be sensitive to being open in the sun, and they may be required to be grown under partial shade during early nursery production. Beauty leaf tree flowers two times per year and up to 8000 fruits per plant can be harvested in a year. It grows best in sandy, well-drained soils. The oil content of beauty leaf seeds is 65%. Beauty leaf oil is a non-edible oil and is dark green in color. As the oil is non-edible, it is considered a second-generation biodiesel feedstock.

Macadamia is a member of the Proteaceous family and is commonly available in New South Wales and central Queensland. Macadamia is also a native Australian tree that can be used to produce biodiesel [28,29]. The color of the seeds are brown, and only the seeds contain oil. The average oil content of the seeds is around 70%, and oils are golden yellow in color [30]. Macadamia oil is an edible oil and that is why it is considered a first generation biodiesel.

3. Materials and Methods

3.1. Materials

Crude macadamia oil was collected from the local market in Rockhampton, and crude beauty-leaf oil was received from a colleague through personal communication. All other chemicals used in this experiment such as methanol, H₂SO₄, CH₄, NaOH, CaCl₂ anhydrous, Na₂SO₄ anhydrous and Whatman filter paper size 150 mm (GE Healthcare Australia Pty. Limited, Parramatta, Sydney, NSW, Australia) were readily available in the chemical laboratory, CQ University, North Rockhampton, Australia.

3.2. Biodiesel Production

The biodiesel production process is traditionally selected based on the acidic value. The two-step acid-base catalyst procedure is needed for a fuel that contains a higher acidic value. For this reason, we measured the acid values of both crude beauty leaf and macadamia oil. The acid values of crude beauty leaf and macadamia oils were found to be 40 mg KOH/g and 4 mg KOH/g oil, respectively. Based on these results, two-step (acid-base catalyst) processes were selected to convert crude beauty-leaf oil, and only the transesterification process has been chosen to convert macadamia oil. The details biodiesel production process can be found in Mofijur et al. [31].

3.3. Characterization of Crude Oils and Biodiesels

The physical and chemical properties of the biodiesels were tested according to ASTM 6751 and EN 14214 standards. Table 1 shows a summary of the equipment and methods used to analyze the properties.

Table 1. Summary of the equipment and method used to analyses the properties.

Property	Equipment	Standard Method	Accuracy
Kinematic Viscosity	NVB Classic (Norma lab, France)	ASTM D445	±0.01 mm ² /s
Density	DM40 LiquiPhysics™ Density Meter (Mettler Toledo, Switzerland)	ASTM D127	±0.1 kg/m ³
Flash Point	NPM 440 Pensky_Martens Flash Point tester (Norma Lab, France)	ASTM D93	±0.1 °C
Cloud and Pour Point	NTE 450 Cloud and Pour Point Tester (Norma Lab, France)	ASTM D2500	±0.1 °C
Acid Number	Automation Titration Rondo 20 (Mettler Toledo, Switzerland)	ASTM D664	0.001 mg KOH/g
Cold Filter Plugging Point (CFPP)	NTE 450 CFPP Tester (Norma Lab, France)	ASTM D6371	±0.1 °C

Cetane number (CN), higher heating value (HHV), iodine value (IV), saponification value (SV), the degree of unsaturation (DU) and long chain saturated factor (LCSF) were calculated from the fatty acid profile of all biodiesel using the following equations described by Mofijur et al. [31]. Table 2 shows the properties of all fuel samples:

$$\text{CN} = 46.3 + (5458/\text{SV}) - (0.225 \cdot \text{IV}), \quad (1)$$

$$\text{SV} = \sum (560 \cdot \text{A}_i) / \text{Mw}_i, \quad (2)$$

$$\text{IV} = \sum (254 \cdot \text{A}_i \cdot \text{D}) / \text{Mw}_i, \quad (3)$$

$$\text{LCSF} = 0.1 \cdot (\text{C16:0, wt. \%}) + 0.5 \cdot (\text{C18:0 wt. \%}) + 1 \cdot (\text{C20:0 wt. \%}) + 1.5 \cdot (\text{C22:0 wt. \%}) + 2.0 \cdot (\text{C24:0 wt. \%}), \quad (4)$$

$$\text{DU} = \sum (\text{Mono Unsaturation Fatty Acids} + 2 \cdot \text{Poly Unsaturation Fatty Acids}), \quad (5)$$

where A_i is the percentage of each component, D is the number of double bonds, and M_{wi} is the molecular mass of each component.

Table 2. Physical and chemical properties of diesel, beauty-leaf biodiesel, and macadamia biodiesel.

Properties	Unit	Method	Macadamia Biodiesel	Beauty Leaf Biodiesel	Australian Diesel
Kinematic Viscosity at 40 °C	mm ² /s	ASTM D445	4.46	4.20	3.23
Density at 15 °C	kg/m ³	ASTM D127	859.2	870	827.2
Higher Heating Value	MJ/kg	ASTM 5468	39.90	39.55	45.30
Oxidation Stability	h	-	3.35	6.82	-
Acid Value	mgKOH/g	ASTM D664	0.07	0.42	-
Flash Point	°C	ASTM D93	178.5	106	68.5
Pour Point	°C	ASTM D2500	0	12	0
Cloud Point	°C	ASTM D2500	8	11	8
CFPP	°C	ASTM D6371	8	-	5
Cetane Number	-	-	56	54	48
Iodine Number	-	-	77.85	85.61	-
Saponification Value	-	-	199	201	-
Long Chain Saturated Factor	-	-	7.24	11.64	-
Degree of Unsaturation	-	-	84.50	94.50	-

3.4. Experimental Setup and Test Procedure

To assess the wear and friction characteristics of beauty leaf and macadamia biodiesel, a four-ball tribotester (TR30H, Ducom Instruments, Chicago, IL, USA) was used in which four stainless-steel type balls were used in this study. Figure 1 shows the schematic diagram of a four ball tribo tester. Table 3 shows details of the tribo tester. Before the beginning of each sample test, all of the steel balls were cleaned using the n-heptane and wiped to dry. All four dry balls were put into a steel cup as an arrangement that three balls were stationary, and another ball was rotating on the stationary balls. After that, 10 mL biodiesel sample was poured into the cup and maintained 3 mL biodiesel depth from the center of the stationary ball surfaces. A WinDucom 2008 software (Version 1, Ducom Instruments, Chicago, IL, USA) connected to the four-ball tester was used to record the frictional torque at different loads (40 kg and 80 kg) and a constant speed (1800 rpm) condition in room temperature according to the ASTM D2796 method. Table 4 shows the operating conditions of tribo-tester. The test was run for a 300 s period, and after each test, the lower three balls were sent for the WSD and SEM/EDX analysis.

Table 3. Details of the four-ball tribo tester.

Specification	Unit	Descriptions	Accuracy
Model	-	TR 30H	-
Speed	RPM	300–3000	±1
Maximum axial load	N	10,000	±0.5
Temperature	°C	Ambient to 100	±0.5
Scar range	Micron	100–4000	±0.5
Test ball (diameter)	mm	12.7	-
Drive motor	kW	1.5	-
Power	V/Hz/VA	380/50/3/2000	-

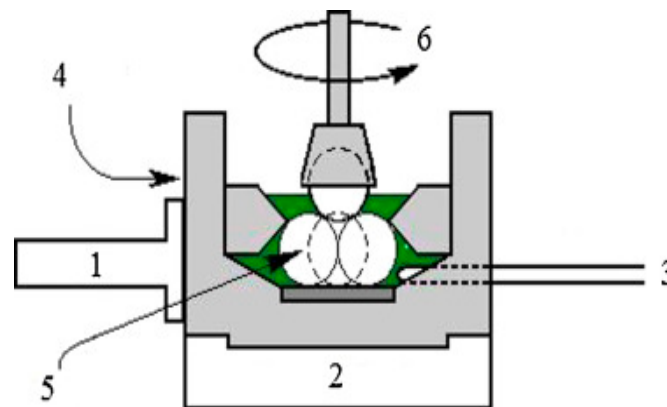


Figure 1. The schematic diagram of the tribo tester (1) Torque arm, (2) Heating zone, (3) Thermocouple, (4) Steel cup, (5) Stationary ball and (6) Rotating ball.

Table 4. Operating conditions of the four-ball tribotester and tested ball specifications.

No.	Parameters	Descriptions
1.	Applied Load (kg)	40, 80
2.	Rotation (RPM)	1800
3.	Fuel Temperature (°C)	27, 45, 60, 75
4.	Test Duration (s)	300
5.	Test Ball Materials	Carbon–chromium steel (SKF)
6.	Composition	10.2% C; 0.45% Si; 0.12% P; 0.07% S; 1.46% Cr; 0.42% Mn; 0.06% Ni; 2.15% Zn and rest 85.06% Fe
7.	Diameter (mm)	12.7
8.	Hardness (HRc)	62
9.	Surface Roughness (µm)	0.1 Centre Line Average in Micrometers (C.L.A)

3.5. Coefficient of Friction

The coefficient of friction was calculated using the following formula. The data of the frictional torque was obtained by applying a load cell.

$$\text{Coefficient of friction (COF), } \mu = \frac{\text{Frictional Torque (kg-mm)} \times \sqrt{6}}{3 \times \text{Applied load (kg)} \times \text{Distance (mm)}} \quad (6)$$

$$= \frac{T\sqrt{6}}{3Wr}$$

where T represents the value of the frictional torque in kg-mm, W represents the applied load in kg, and r is the distance in mm.

3.6. Flash Temperature Parameter (FTP)

Flash temperature parameter was first introduced by Lane [32] in 1957. It is the temperature at which oil creates the lubricating films to provide the lubricity. The higher FTP indicates the better lubrication performance, whereas the lower FTP indicates lower lubrication performance. At lower FTP, the lubrication films are broken down and that is why lubrication performance is poor [33]. In this study, the FTP was calculated using the following formula:

$$\text{Flash temperature parameter, FTP} = \frac{\text{Applied load}}{(\text{Wear scan diameter})^{1.4}} \quad (7)$$

$$= \frac{W}{d^{1.4}}$$

where W indicates the applied load in kg, and d is the value of the wear scar diameter (WSD) in mm.

3.7. Wear Evaluation

An optical microscope model, C2000 (IKA, Wilmington, DE, USA) with a 0.01 mm resolution, was used to measure the WSD of the tested balls (according to the ASTM D4172 method). The wear scar images of the balls were captured, and the wear scar diameter was measured using the computer software. After each test, the value of the wear scar diameter of all balls was averaged. The same procedure was maintained for all biodiesel samples.

3.8. SEM/EDX Analysis

An SEM analyzer used to analyze the worn scar surfaces of tested balls. For SEM/EDX analysis, the samples were sent to a Quasi-s lab, UKM, Wanyi, Selangor, Malaysia. SEM/EDX analysis was conducted using a Hitachi S4500 SEM analyzer (Newport News, VA, USA). In this study, the topographic images of a sample were produced by scanning that focused on the worn scar surface area by a beam of electrons. The electron beam is scanned in a raster scar surface, and the beam's position is combined with the detected signal to produce an image. The energy-dispersive X-ray spectroscopy (EDS, EDX, or XEDS) was used to analyses the metal elements or chemical characteristics of worn scar surface areas.

3.9. Error Analysis

The experimental results are associated with a series of tasks such as observation, instruments selection, data collection, and calibrations. Thus, some errors (the difference between a measurement and the true value of the measurand) and uncertainties may be present in the experimental results, and it is imperative to do the error analysis to judge the accuracy (the closeness of agreement between a measured value and the true value) of the test. Statistical analysis was performed by using a two-tailed paired *t*-test for independent variables to test the significant differences among the sample set means using Microsoft Excel 2013 (Sydney, NSW, Australia). Data were collected at least three times and averaged to perform graph plotting to perform precision measuring. A sample error calculation of FTP for beauty leaf biodiesel has been provided in Table 5.

Table 5. Summary of relative uncertainty and accuracy for experimental results.

Condition	1st Data	2nd Data	3rd Data	max	min	Accuracy		Average	Error
						+1	−1		
L40_27	127.58	113.59	131.10	131.10	113.59	132.10	112.59	122.34	±0.07
L40_T55	132.92	110.83	129.32	132.92	110.83	133.92	109.83	121.87	±0.09
L40_T75	69.80	73.64	82.50	82.50	69.80	83.50	68.80	76.15	±0.08
L80_27	21.79	25.10	22.79	25.10	21.79	26.10	20.79	23.45	±0.07
L80_T55	19.70	20.49	20.72	20.72	19.70	21.72	18.70	20.21	±0.03
L80_T75	17.23	20.23	20.77	20.77	17.23	21.77	16.23	19.00	±0.09

4. Results and Discussion

4.1. Friction Characteristics of Biodiesel Fuels

The COF was calculated in two conditions, namely unsteady state condition and stable condition. When the experiment starts, the COF of both biodiesel is not stable, and it takes a few minutes to become stable [21]. This is why it is called an unsteady state condition, and the later state is known as a stable condition. The unsteady state condition is also known as the run-in period [21]. However, the friction characteristics of both first generation and second generation biodiesel in both the unsteady state and steady state conditions are discussed as follows.

4.1.1. Friction Characteristics at Different Load and Run-In Periods (Unsteady State Condition)

The COF of any fuel represents the lubrication characteristics of that particular fuel. Figure 2a demonstrates the coefficient of friction of biodiesel fuel in an unsteady state at a 40 kg load. It is seen that in the unsteady state condition, diesel fuel has the highest COF compared to both first and second generation biodiesel. Both beauty leaf biodiesel and macadamia biodiesel lowers the COF by 76.60% and 83.48%, respectively, compared to diesel fuel. The maximum COFs for diesel fuel, macadamia and beauty leaf biodiesel were found to be 4 s, 2.9 s, and 2 s respectively. Figure 2b displays the COF of biodiesel fuel in an unsteady state condition at an 80 kg load. When the load increases from 40 kg to 80 kg, the COFs of all tested fuels also increase. It is clear that at higher load conditions, the lowest COF was found for macadamia biodiesel followed by the beauty leaf biodiesel and diesel fuel. Similar trends on the results of COFs at lower load conditions were also found for higher load conditions. Both macadamia biodiesel and beauty leaf biodiesel lower the COF by 75.28% and 61.18%, respectively, compared to the diesel fuel. The results of lower COF for biodiesel can be explained by the ester contents of biodiesel, which has more scuffing protection quality compared to diesel [34]. The ester of biodiesel fuel helps rapid changes from the unsteady to steady conditions. It was reported that the palm biodiesel blends reduce the run-in period faster than the diesel fuel [20]. Habibullah et al. [35] also found less run-in period for calophyllum biodiesel blends. In the run-in period at lower load conditions, macadamia biodiesel lowered its COF by 29.42% compared to beauty leaf biodiesel, whereas, at higher load condition, macadamia biodiesel lowered its COF by 36.32% more than beauty leaf biodiesel. In addition, the lower COF of biodiesel can be described by the lubricating oil film from the maximum adsorbed long-chained polar molecules on the friction surfaces [36]. The presence of sulfur and oxygen in the biodiesel is considered a major part of producing the lubricating films. Thus, biodiesel fuels have a superb lubrication performance and lower the friction compared to that of diesel fuel at both 40 kg and 80 kg load conditions.

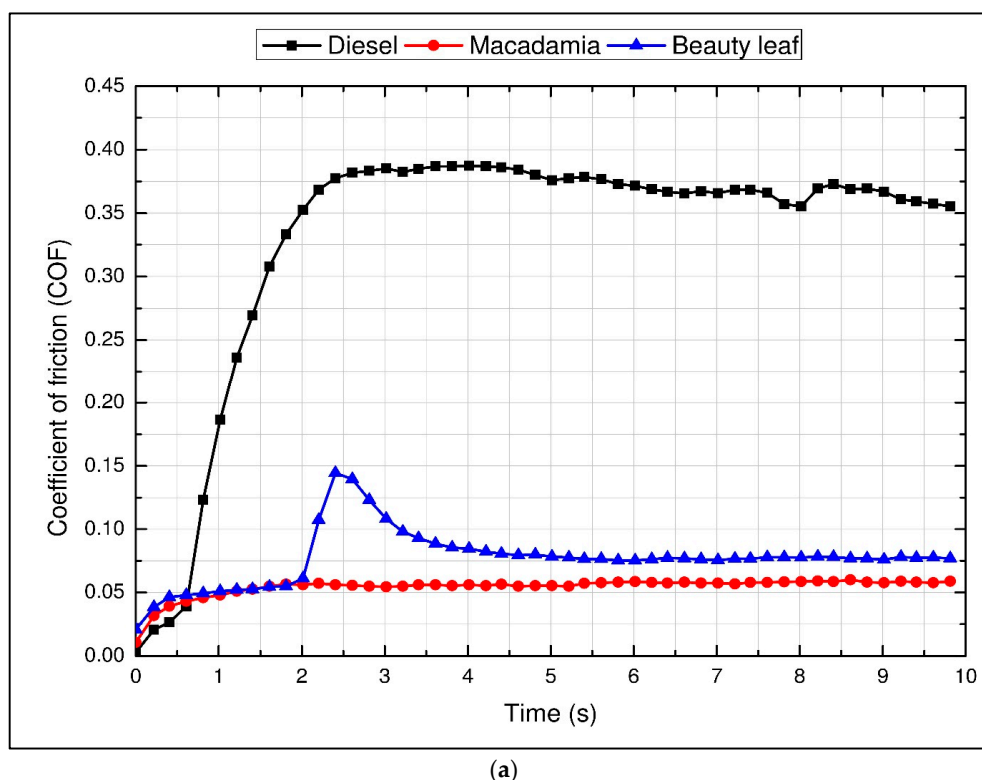


Figure 2. Cont.

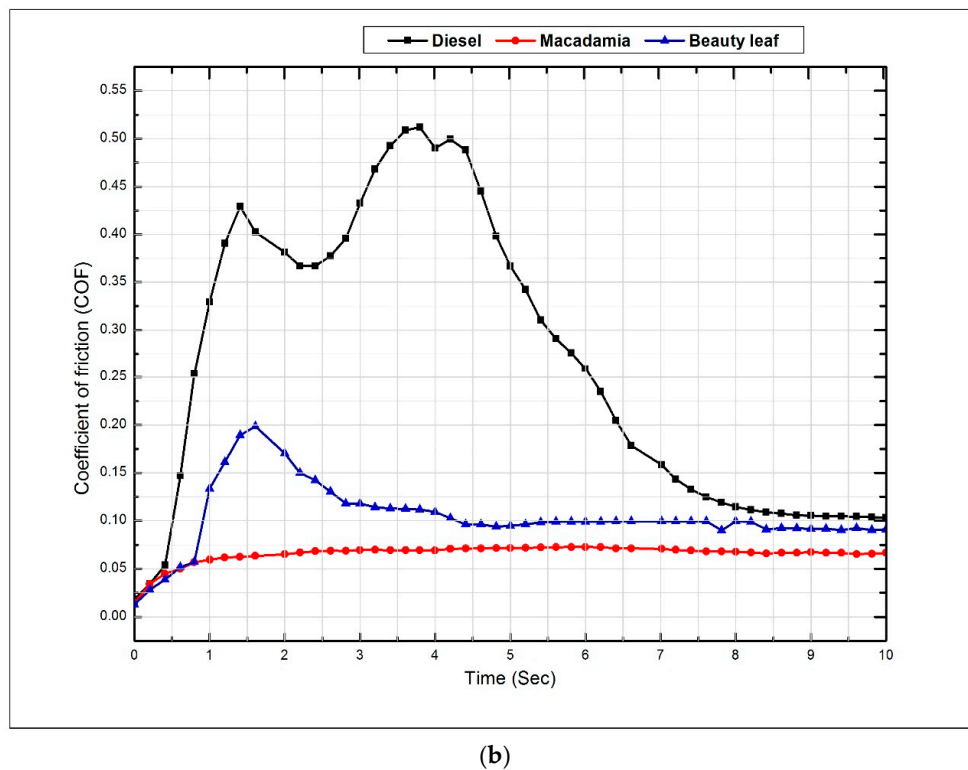


Figure 2. The variation of COFs of biodiesel in unsteady state conditions (a) in a 40 kg load condition and (b) in an 80 kg load condition.

4.1.2. Friction Characteristics at Different Loads and Steady State Conditions

Figure 3a shows the COF of all fuel samples at 40 kg load and in steady state condition. It is seen that biodiesel lowers the steady-state COF compared to diesel fuel. All biodiesel fuels displayed similar COF trends for longer time periods, whereas the COF of diesel fuel suddenly rose at 250 s and then sharply declined. The highest COF value for diesel, macadamia and beauty leaf biodiesel was found to be 0.42, 0.08 and 0.09 at 250 s, 220 s, and 245 s, respectively. In a steady-state condition, the maximum average COF was found to be 0.35 for diesel followed by the beauty leaf (0.08) and macadamia biodiesel (0.07). The macadamia biodiesel and beauty leaf biodiesel lower the COF by 79.21% and 76.41%, respectively.

Figure 3b shows the COFs of all fuel samples at 80 kg load and steady state conditions. It is seen that all the fuels show a similar trend in the lower load conditions. In higher load conditions, diesel fuel showed the highest COF than macadamia and beauty leaf biodiesel. The maximum COF value for diesel, macadamia and beauty leaf biodiesel was found to be 0.10, 0.08 and 0.07 at 297 s, 237 s and 247 s, respectively. In a steady-state condition, the maximum average COF was found to be 0.09 for diesel followed by the beauty leaf (0.07) and macadamia biodiesel (0.06). The macadamia biodiesel and beauty leaf biodiesel lowered their COFs by 21.67% and 11.71%, respectively. In an 80 kg load condition, the COF of macadamia biodiesel increased suddenly, held for a couple of seconds, and then decreased gradually over time. In all of the load conditions, biodiesel fuels displayed a lower steady state COF than diesel fuel. These results can be explained by the oxygen containing compounds such as free fatty acids and esters that play a friction reducing role. These compounds immersed or responded on the chafing metal surfaces and decreased the bond between the enclosing asperities for rubbing and wear seizure [37].

Between the biodiesel fuels, macadamia biodiesel lowered the steady-state COF in lower load conditions and also in higher load conditions. The macadamia biodiesel lowered COF by 11.86% in lower load condition and 12.72% in higher load conditions, respectively. The lower COF of biodiesel

fuel in the steady state condition can be credited to the higher degree of unsaturated fatty acid compositions [38,39]. The presence of a large number of unsaturated compounds in the methyl ester reduces the friction. In addition, biodiesel fuel contains polyunsaturated compounds that form the protective film [40]. The fatty acid composition results showed that macadamia biodiesel has higher unsaturated fatty acid (82.60%) compared to the beauty leaf biodiesel (64.6%). In particular, the unsaturated compound oleic acid mainly plays the role of lowering the friction. The oleic acid was found to be 61.3% for macadamia biodiesel and 38.2% for beauty leaf biodiesels.

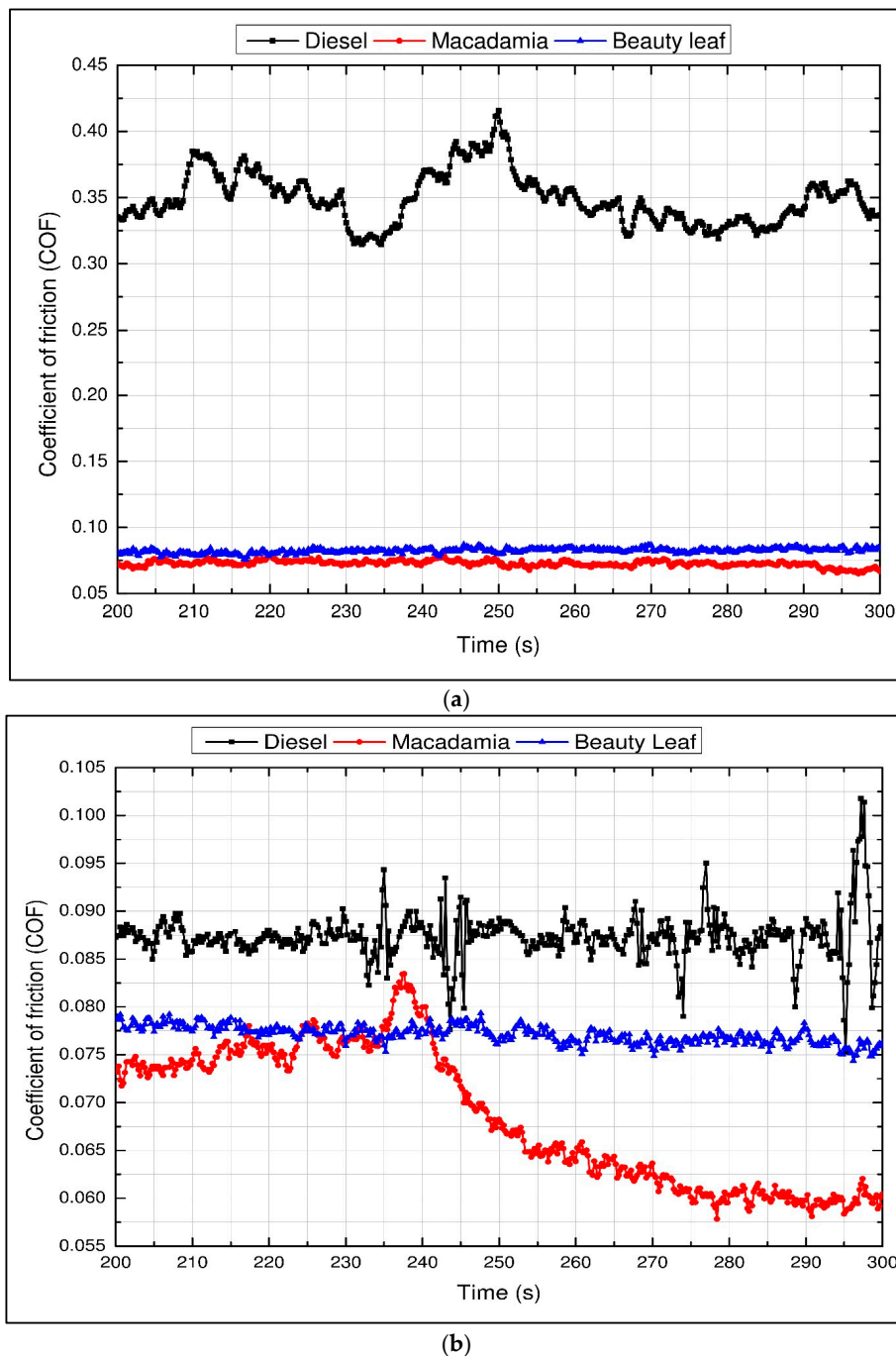


Figure 3. The variation of COFs of biodiesel in steady state conditions (a) in a 40 kg load condition and (b) in a 80 kg load condition.

4.2. Wear Characteristics of Biodiesel Fuels at Different Loads and Temperatures

The impact of different loads and temperatures on WSD of all of the different samples are shown in Figure 4 and Table 6. It is seen that the WSD is increased for all the fuel samples with the variations of both load and temperature. The results can be explained by the contact pressure between the metal contact surfaces of the experimental ball. Syahrullail et al. [41] reported that the larger WSD causes more wear and worn scar surfaces. In addition, the oxidation in the biodiesel sample is likely to break down the tribological properties of the material. The degeneration of oxidation can be done by removing the metallic soap film formation through a higher wear load [42].

The diesel fuel showed the highest average WSD followed by the macadamia and beauty leaf biodiesel. On average, the beauty leaf biodiesel and macadamia biodiesel lowers the WSD at lower loads by 41.28% and 19.35%, respectively. At higher loads, the reduction of WSD for the beauty leaf biodiesel and macadamia biodiesel was found to be 27.29% and 28.60%, respectively. The lowest amount of WSD was found for beauty leaf biodiesel (0.27294 mm) at a 40 kg load and at room temperature (27 °C). The pure palm biodiesel lowered WSD compared to diesel fuel at different speed conditions [20]. The pure calophyllum biodiesel lowers the average WSD more than diesel and other biodiesel in different load conditions. The presence of trace elements in biodiesel containing methyl ester, free fatty acids, triglycerides and mono-glycerides in the biodiesel, which enhance the lubricity of biodiesel, is expected [43]. Among the biodiesels, the beauty leaf biodiesel showed lower WSD than macadamia biodiesel at all loads and temperature. On average, the beauty leaf biodiesel lowered WSD by 27.18% and 1.79% at 40 kg and 80 kg loads, respectively.

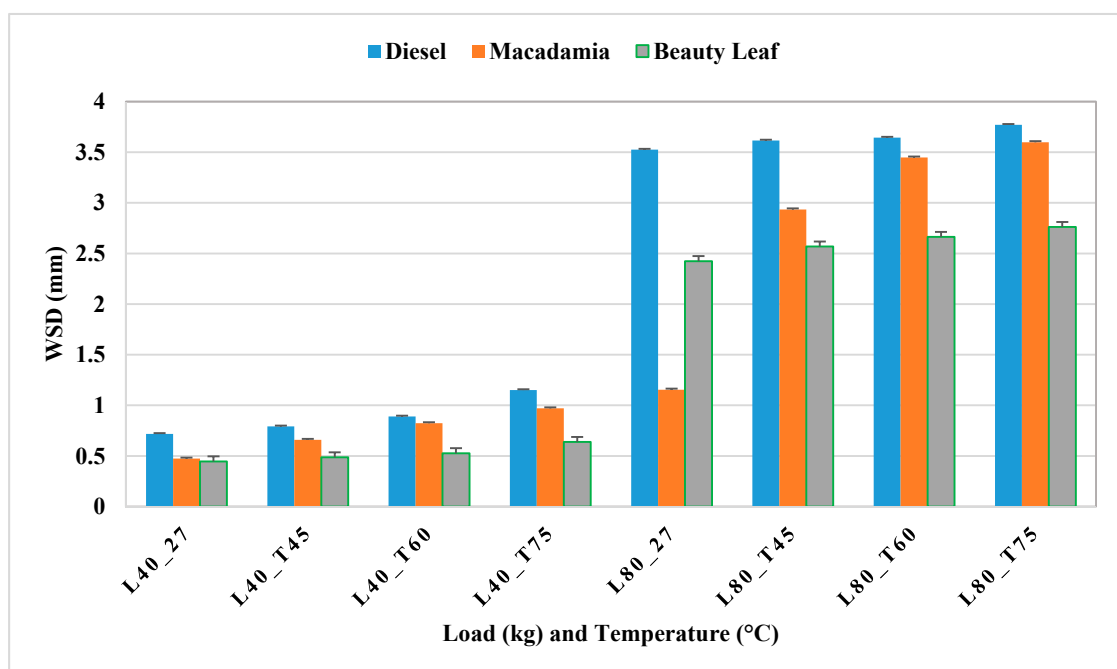


Figure 4. The variations of WSD of all samples at different loads.

4.3. Flash Parameter Temperature at Different Loads and Temperatures

The FTPs of all samples at different loads and temperatures are shown in Figure 5 and Table 6. The FTP of all samples decreased with an increase in the frictional loads and temperatures. Unlikely the WSD, when the applied loads were increased, caused a decreased in FTPs.

The highest average FTP was found for beauty leaf biodiesel followed by the macadamia biodiesel and diesel in 40 kg load conditions. However, at higher loads, the highest average FTP was found for macadamia biodiesel followed by the beauty leaf biodiesel and diesel. On average, the diesel and

macadamia biodiesel lowered the FTP at lower loads by 51% and 31.22%, respectively, compared to beauty leaf biodiesel. However, at higher loads, diesel and beauty leaf biodiesel lowered the FTP by 52.5% and 23.95%, respectively, compared to macadamia biodiesel. Compared to all samples the maximum FTP was observed for beauty leaf biodiesel (123.68) at 40 kg load and room temperature (27 °C). The minimum FTP value was observed for diesel (12.48) at 80 kg load and 75 °C temperature. The DU of biodiesel fuels maximizes the lubrication performance [44]. In addition, the oxidation process has an impact on the lubrication performance. For example, the oxidation progression offers better lubrication performance in short period tests, whereas in longer period tests, it causes fuel degradation and corrosion in the metal surfaces [16]. Biodiesels are oxidized due to the unsaturated fatty acids, impurities presented in the biodiesel, light, temperature, and humidity.

Table 6. Flash Temperature Parameter of macadamia and beauty leaf biodiesel.

Fuel	Load 40 kg				Load 80 kg			
	27 °C	45 °C	60 °C	75 °C	27 °C	45 °C	60 °C	75 °C
Diesel	63.60	55.39	47.07	32.87	13.71	13.23	13.08	12.48
Macadamia Biodiesel	113.59	71.73	52.54	41.74	65.41	17.71	14.14	13.32
Beauty Leaf Biodiesel	123.68	109.68	98.20	75.00	23.16	21.35	20.29	19.30

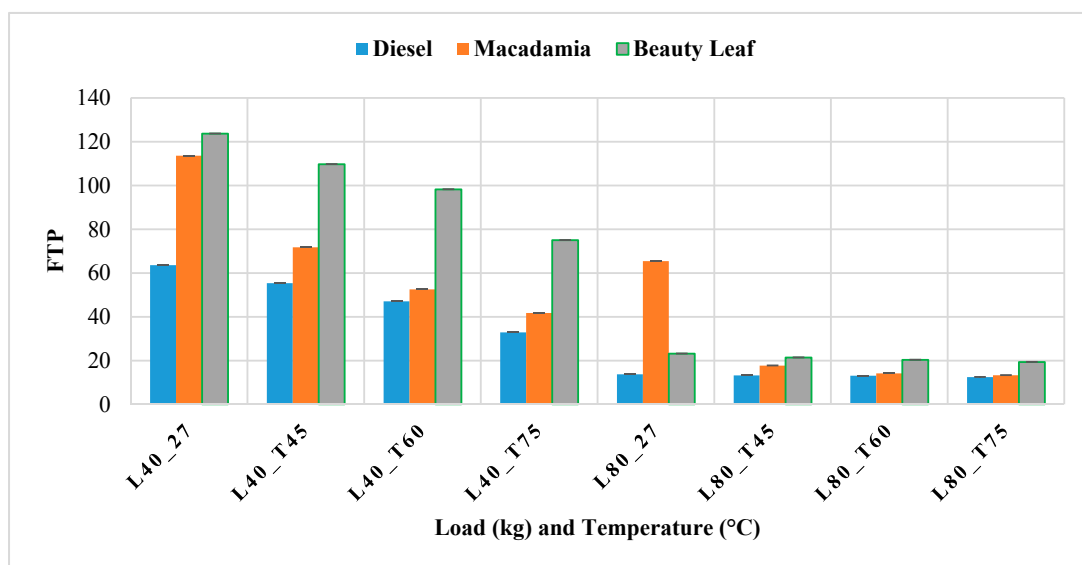


Figure 5. The FTPs of different fuels under different loads and temperatures.

4.4. Analysis of SEM/EDX

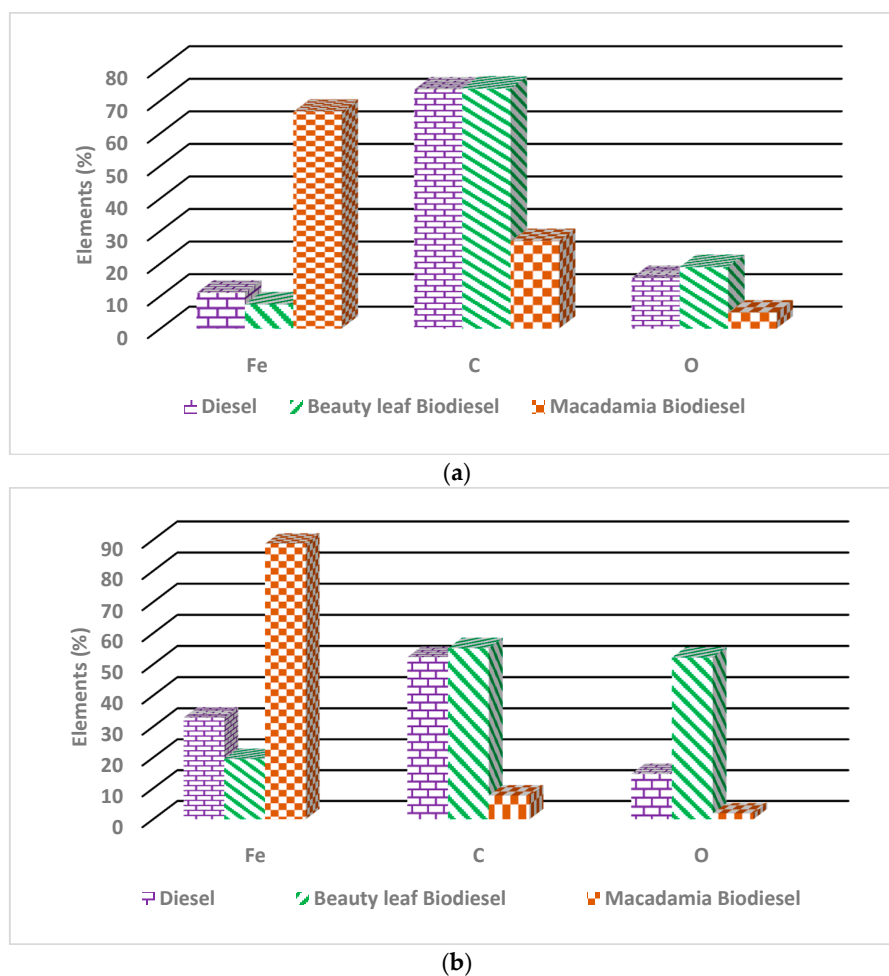
4.4.1. Analysis of Filtering Metal Debris by SEM/EDX

At the end of the test, all of the samples were filtered using a good quality filter paper to collect metal debris for SEM/EDX analysis. Through the SEM/EDX analysis, the iron (Fe), carbon (C) and oxygen (O) were spotted on different locations of the filter paper and showed in weight percentage and atomic percentage. Table 7 displays the filtering debris data of all samples.

Table 7. Filtering metal debris analysis.

Elements	Diesel	Beauty Leaf Biodiesel	Macadamia Biodiesel
Metals elements in weight (%)			
Fe	32.93	19.55	88.95
C	52.34	55.52	8.70
O	14.73	24.93	2.35
Metal elements in atomic (%)			
Fe	11.01	7.43	67.89
C	73.46	73.72	26.88
O	15.53	18.92	5.23

The analysis of filtering particle debris using an SEM/EDX analysis curve is also shown in Figure 6a,b. The minimum percentage of C and O was present in macadamia biodiesel fuel compared to diesel and other biodiesels. Macadamia biodiesel contained the maximum amount of Fe compared to diesel and beauty leaf biodiesel in both atomic and weight percentages. The highest C and O elements in both atomic and weight percentages were found in beauty leaf biodiesel followed by the diesel and macadamia biodiesel. The higher contents of O in beauty leaf biodiesel could offer better lubrication performance by producing iron oxide on the solid surfaces [33,45]. Hence, beauty-leaf biodiesel showed favorable lubrication performance based on the SEM/EDX analysis results.

**Figure 6.** The analysis of filtering particle debris (a) weight percentages (b) atomic percentages.

4.4.2. Analysis of Worn Surfaces by SEM/EDX

The worn scar surface investigation is important for finding the metallic failures that occurred due to the effect of friction and wear between the contact surfaces. The SEM analysis of the stationary steel balls used in this study in higher load conditions is depicted in Figure 7. The worn scar surface areas of the stationary ball for diesel were 27.92% and 2.20% higher than beauty leaf and macadamia biodiesel, respectively. Diesel fuel showed the highest surface deformation compared to beauty leaf and macadamia biodiesel. Mosarof et al. [33] also found similar results for palm and calophyllum biodiesel blends. The results of lower worn scar surface for biodiesel can be explained by the presences of ester molecules that formed a monolayer film between the metal contact faces, thus improving the lubricity of the biodiesel samples [35]. In addition, the higher oxygen content of biodiesel compared to diesel fuel produced more inorganic oxides (such as; FeS, Fe₂O₃) in the lubricating film [33]. It was found that the surface damage of the experimental ball damaged is larger than 20 μm, which indicates that the damage was due to adhesive wear. Apart from this, the circular, tiny and steady scuffs on the ball characterize abrasive wear [46]. Macadamia biodiesel, beauty leaf biodiesel and diesel formed cracks on the test ball shells due to the corrosive wear as shown in Figure 7(b1,c1), (b2,c2) and (b3,c3). The reason for corrosive wear can be explained by the existence of acidic compounds in biodiesel that led to the corrosive wear in contact surfaces of the tested balls. The cracks on the worn surfaces of the ball were formed due to the irregular malleable distortion at high loads. The black spots on the worn surfaces in Figure 7(a1,a3) reflected the oxidative corrosion that was caused by the various acids and peroxides [33].

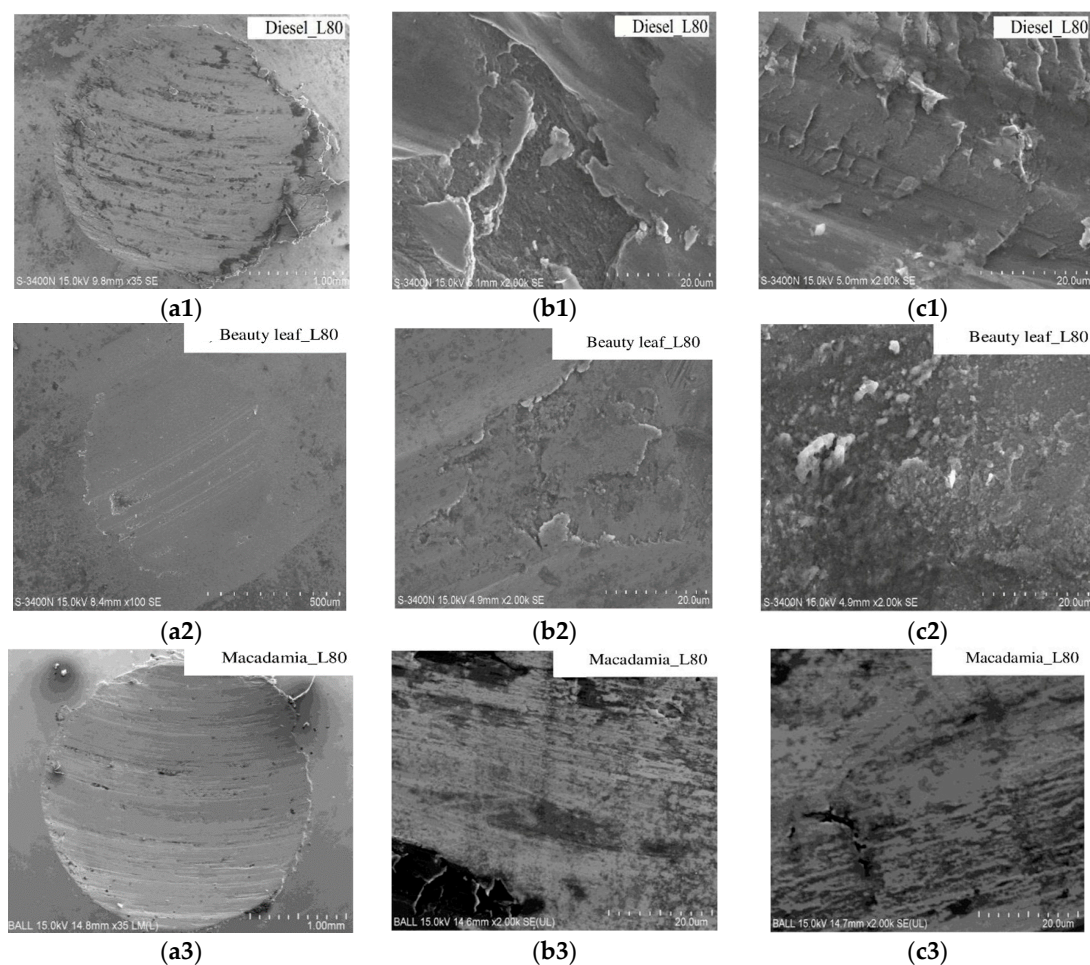


Figure 7. SEM analysis of worn scar surfaces for steel balls at 80 kg load.

5. Conclusions

This study compared the tribological characteristics of Australian native first and second generation biodiesels with diesel fuel. The following conclusions can be drawn based on this study.

In the run-in period and steady state conditions, both biodiesels offered lower COFs (15% to 83.5%) compared to diesel fuel under the variation of loads. This can be explained by the presence of ester in biodiesel, which shows better scuffing protection characteristics than diesel.

WSD analysis results showed that both biodiesels lower the WSD by 19.65% to 41.28% compared to the diesel fuel, depending on the load. The FTP results indicated that biodiesel fuels have higher FTP (up to 52%) than diesel fuel, depending on the load. This can be explained by the oxidation in biodiesel that enhances the lubrication performance.

SEM/EDX analysis results showed that biodiesel fuel has a minimum percentage of C and O, except for Fe, compared to diesel. In addition, diesel fuel has the highest surface deformation compared to biodiesel fuel. The worn scar surface area of the steel ball for diesel was found (2.20%–27.92%) to be higher than biodiesel.

The findings of the present study indicate that both first and second generation biodiesel fuel have better tribological performance than diesel fuel, and, among the biodiesels, macadamia biodiesel showed better lubrication performance. Thus, according to the tribological property results, biodiesel can be used as a fuel in diesel engines to reduce the wear of the engine.

Acknowledgments: This work was conducted under an International Postgraduate Research Award (IPRA) Scholarship funded by the Central Queensland University, Rockhampton, Australia.

Author Contributions: The contributions of each author are as follows: Md Mofijur Rahman produced biodiesel, collected experimental data, analysed the numerical results, drafted and revised the manuscript; Mohammad Rasul contributed to the experimental design and thoroughly revised the paper; Nur Mohammad Sayeed Hassan helped to revise the paper according to the reviewer comments.

Conflicts of Interest: The authors declare no conflict of interest.

References

1. Hassan, N.M.S.; Rasul, M.G.; Harch, C.A. Modelling and experimental investigation of engine performance and emissions fuelled with biodiesel produced from Australian beauty leaf tree. *Fuel* **2015**, *150*, 625–635. [[CrossRef](#)]
2. Mofijur, M.; Masjuki, H.H.; Kalam, M.A.; Hazrat, M.A.; Liaquat, A.M.; Shahabuddin, M.; Varman, M. Prospects of biodiesel from jatropha in Malaysia. *Renew. Sustain. Energy Rev.* **2012**, *16*, 5007–5020. [[CrossRef](#)]
3. Mofijur, M.; Rasul, M.G.; Hassan, N.M.S.; Masjuki, H.H.; Kalam, M.A.; Mahmudul, H.M. Assessment of physical, chemical and tribological properties of different biodiesel fuel. In *Clean Energy for Sustainable Development*; Rasul, M., Ed.; Elsevier: Amsterdam, The Netherlands, 2016; Volume 1, pp. 441–461.
4. Mofijur, M.; Rasul, M.G.; Hyde, J.; Azad, A.K.; Mamat, R.; Bhuiya, M.M.K. Role of biofuel and their binary (diesel–biodiesel) and ternary (ethanol–biodiesel–diesel) blends on internal combustion engines emission reduction. *Renew. Sustain. Energy Rev.* **2016**, *53*, 265–278. [[CrossRef](#)]
5. Harch, C.A.; Rasul, M.G.; Hassan, N.M.S.; Bhuiya, M.M.K. Modelling of engine performance fuelled with second generation biodiesel. *Procedia Eng.* **2014**, *90*, 459–465. [[CrossRef](#)]
6. Dai, Y.-M.; Wu, J.-S.; Chen, C.-C.; Chen, K.-T. Evaluating the optimum operating parameters on transesterification reaction for biodiesel production over a LiAlO₂ catalyst. *Chem. Eng. J.* **2015**, *280*, 370–376. [[CrossRef](#)]
7. Dai, Y.-M.; Chen, K.-T.; Chen, C.-C. Study of the microwave lipid extraction from microalgae for biodiesel production. *Chem. Eng. J.* **2014**, *250*, 267–273. [[CrossRef](#)]
8. Rashed, M.M.; Kalam, M.A.; Masjuki, H.H.; Mofijur, M.; Rasul, M.G.; Zulkifli, N.W.M. Performance and emission characteristics of a diesel engine fueled with palm, jatropha, and moringa oil methyl ester. *Ind. Crops Prod.* **2016**, *79*, 70–76. [[CrossRef](#)]
9. Azad, A.K.; Rasul, M.G.; Khan, M.M.K.; Sharma, S.C.; Mofijur, M.; Bhuiya, M.M.K. Prospects, feedstocks and challenges of biodiesel production from beauty leaf oil and castor oil: A nonedible oil sources in Australia. *Renew. Sustain. Energy Rev.* **2016**, *61*, 302–318. [[CrossRef](#)]

10. Ali, O.M.; Mamat, R.; Abdullah, N.R.; Abdullah, A.A. Analysis of blended fuel properties and engine performance with palm biodiesel–diesel blended fuel. *Renew. Energy* **2016**, *86*, 59–67. [[CrossRef](#)]
11. Mofijur, M.; Masjuki, H.H.; Kalam, M.A.; Ashrafur Rahman, S.M.; Mahmudul, H.M. Energy scenario and biofuel policies and targets in ASEAN countries. *Renew. Sustain. Energy Rev.* **2015**, *46*, 51–61. [[CrossRef](#)]
12. Bhuiya, M.M.K.; Rasul, M.G.; Khan, M.M.K.; Ashwath, N.; Azad, A.K.; Hazrat, M.A. Prospects of 2nd generation biodiesel as a sustainable fuel—Part 2: Properties, performance and emission characteristics. *Renew. Sustain. Energy Rev.* **2016**, *55*, 1129–1146. [[CrossRef](#)]
13. Sarin, A.; Arora, R.; Singh, N.P.; Sarin, R.; Malhotra, R.K.; Sharma, M.; Khan, A.A. Synergistic effect of metal deactivator and antioxidant on oxidation stability of metal contaminated Jatropha biodiesel. *Energy* **2010**, *35*, 2333–2337. [[CrossRef](#)]
14. Fazal, M.A.; Haseeb, A.S.M.A.; Masjuki, H.H. Biodiesel feasibility study: An evaluation of material compatibility; performance; emission and engine durability. *Renew. Sustain. Energy Rev.* **2011**, *15*, 1314–1324. [[CrossRef](#)]
15. Jain, S.; Sharma, M.P. Stability of biodiesel and its blends: A review. *Renew. Sustain. Energy Rev.* **2010**, *14*, 667–678. [[CrossRef](#)]
16. Haseeb, A.S.M.A.; Sia, S.Y.; Fazal, M.A.; Masjuki, H.H. Effect of temperature on tribological properties of palm biodiesel. *Energy* **2010**, *35*, 1460–1464. [[CrossRef](#)]
17. Muñoz, M.; Moreno, F.; Monné, C.; Morea, J.; Terradillos, J. Biodiesel improves lubricity of new low sulphur diesel fuels. *Renew. Energy* **2011**, *36*, 2918–2924. [[CrossRef](#)]
18. Ozioko, F.U. Synthesis and study of properties of biolubricant based on *Moringa oleifera* oil for industrial application. *AU J. Technol.* **2009**, *17*, 137–142.
19. Sharma, B.K.; Rashid, U.; Anwar, F.; Erhan, S.Z. Lubricant properties of Moringa oil using thermal and tribological techniques. *J. Therm. Anal. Calorim.* **2009**, *96*, 999–1008. [[CrossRef](#)]
20. Fazal, M.A.; Haseeb, A.S.M.A.; Masjuki, H.H. Investigation of friction and wear characteristics of palm biodiesel. *Energy Convers. Manag.* **2013**, *67*, 251–256. [[CrossRef](#)]
21. Habibullah, M.; Masjuki, H.H.; Kalam, M.A.; Zulkifli, N.W.M.; Masum, B.M.; Arslan, A.; Gulzar, M. Friction and wear characteristics of *Calophyllum inophyllum* biodiesel. *Ind. Crops Prod.* **2015**, *76*, 188–197. [[CrossRef](#)]
22. Wain, K.S.; Perez, J.M.; Chapman, E.; Boehman, A.L. Alternative and low sulfur fuel options: Boundary lubrication performance and potential problems. *Tribol. Int.* **2005**, *38*, 313–319. [[CrossRef](#)]
23. Kumar, N.; Chauhan, S. Analysis of tribological performance of biodiesel. *Proc. Inst. Mech. Eng. Part J J. Eng. Tribol.* **2014**, *228*, 797–807. [[CrossRef](#)]
24. Maru, M.M.; Trommer, R.M.; Cavalcanti, K.F.; Figueiredo, E.S.; Silva, R.F.; Achete, C.A. The stribeck curve as a suitable characterization method of the lubricity of biodiesel and diesel blends. *Energy* **2014**, *69*, 673–681. [[CrossRef](#)]
25. Sulek, M.W.; Kulczycki, A.; Malysa, A. Assessment of lubricity of compositions of fuel oil with biocomponents derived from rape-seed. *Wear* **2010**, *268*, 104–108. [[CrossRef](#)]
26. Sanjid, A.; Masjuki, H.H.; Kalam, M.A.; Rahman, S.M.A.; Abedin, M.J.; Palash, S.M. Impact of palm, mustard, waste cooking oil and *Calophyllum inophyllum* biofuels on performance and emission of CI engine. *Renew. Sustain. Energy Rev.* **2013**, *27*, 664–682. [[CrossRef](#)]
27. Ashwath, N. *Evaluating Biodiesel Potential of Australian Native and Naturalised Plant Species*; Rural Industries Research and Development Corporation: Kingston, Australia, 2010.
28. The Bopple Nut. Mount Bauple & District Historical Society Inc. Available online: <http://www.bauplemuseum.com/bopple%20nut%20pub.pdf> (accessed on 30 December 2015).
29. Macadamia. Australian Plant Name Index (APNI), Integrated Botanical Information System (IBIS) Database (Listing by % Wildcard Matching of all Taxa Relevant to Australia). Available online: <https://biodiversity.org.au/nsl/services/apni?name=Macadamia%25&max=100&display=apni&search=true> (accessed on 30 December 2015).
30. Knothe, G. Biodiesel derived from a model oil enriched in palmitoleic acid, macadamia nut oil. *Energy Fuels* **2010**, *24*, 2098–2103. [[CrossRef](#)]
31. Rahman, M.; Rasul, M.; Hassan, N.; Hyde, J. Prospects of biodiesel production from macadamia oil as an alternative fuel for diesel engines. *Energies* **2016**, *9*, 403. [[CrossRef](#)]
32. Lane, T.B. The flash temperature parameter: A criterion for assessing EP performance in the four-ball machine. *J. Inst. Pet.* **1957**, *43*, 181–188.

33. Mosarof, M.H.; Kalam, M.A.; Masjuki, H.H.; Alabdulkarem, A.; Habibullah, M.; Arslan, A.; Monirul, I.M. Assessment of friction and wear characteristics of *Calophyllum inophyllum* and palm biodiesel. *Ind. Crops Prod.* **2016**, *83*, 470–483. [[CrossRef](#)]
34. Konishi, T.; Klaus, E.; Duda, J. Wear characteristics of aluminum-silicon alloy under lubricated sliding conditions. *Tribol. Trans.* **1996**, *39*, 811–818. [[CrossRef](#)]
35. Habibullah, M.; Masjuki, H.H.; Kalam, M.A.; Gulzar, M.; Arslan, A.; Zahid, R. Tribological characteristics of *Calophyllum inophyllum*-based TMP (trimethylolpropane) ester as energy-saving and biodegradable lubricant. *Tribol. Trans.* **2015**, *58*, 1002–1011. [[CrossRef](#)]
36. Xu, Z.; Shi, X.; Zhai, W.; Yao, J.; Song, S.; Zhang, Q. Preparation and tribological properties of TiAl matrix composites reinforced by multilayer graphene. *Carbon* **2014**, *67*, 168–177. [[CrossRef](#)]
37. Adebisi, A.A.; Maleque, M.A. Modelling aspect of corrosive wear under biodiesel. In Proceedings of the Regional Tribology Conference, Langkawi Island, Malaysia, 22–24 November 2011; Volume 6, pp. 161–168.
38. Martín-Alfonso, J.E.; Valencia, C. Tribological, rheological, and microstructural characterization of oleogels based on EVA copolymer and vegetables oils for lubricant applications. *Tribol. Int.* **2015**, *90*, 426–434. [[CrossRef](#)]
39. Rani, S.; Joy, M.L.; Nair, K.P. Evaluation of physiochemical and tribological properties of rice bran oil—Biodegradable and potential base stock for industrial lubricants. *Ind. Crops Prod.* **2015**, *65*, 328–333. [[CrossRef](#)]
40. Asadauskas, S.; Perez, J.M.; Duda, J.L. Oxidative stability and antiwear properties of high oleic vegetable oils. *Lubr. Eng.* **1996**, *52*, 877–882.
41. Syahrullail, S.; Wira, J.Y.; Wan Nik, W.; Fawwaz, W. Friction characteristics of RBD palm olein using four-ball tribotester. *Appl. Mech. Mater.* **2013**, *315*, 936–940. [[CrossRef](#)]
42. Jayadas, N.H.; Prabhakaran Nair, K.; Ajithkumar, G. Tribological evaluation of coconut oil as an environment-friendly lubricant. *Tribol. Int.* **2007**, *40*, 350–354. [[CrossRef](#)]
43. Hu, J.; Du, Z.; Li, C.; Min, E. Study on the lubrication properties of biodiesel as fuel lubricity enhancers. *Fuel* **2005**, *84*, 1601–1606. [[CrossRef](#)]
44. Geller, D.P.; Goodrum, J.W. Effects of specific fatty acid methyl esters on diesel fuel lubricity. *Fuel* **2004**, *83*, 2351–2356. [[CrossRef](#)]
45. Mosarof, M.H.; Kalam, M.A.; Masjuki, H.H.; Alabdulkarem, A.; Ashraful, A.M.; Arslan, A.; Rashedul, H.K.; Monirul, I.M. Optimization of performance, emission, friction and wear characteristics of palm and *Calophyllum inophyllum* biodiesel blends. *Energy Convers. Manag.* **2016**, *118*, 119–134. [[CrossRef](#)]
46. Sperring, T.; Nowell, T. Syclops—A qualitative debris classification system developed for RAF early failure detection centres. *Tribol. Int.* **2005**, *38*, 898–903. [[CrossRef](#)]



© 2017 by the authors; licensee MDPI, Basel, Switzerland. This article is an open access article distributed under the terms and conditions of the Creative Commons Attribution (CC-BY) license (<http://creativecommons.org/licenses/by/4.0/>).